

Supporting Information

Efficient utilization of carbon to produce aromatic valencene in *Saccharomyces cerevisiae* using mannitol as substrate

Chaoyi Zhu^a, Xia You^a, Tao Wu^a, Wen Li^a, Hefeng Chen^a, Yaping Cha^a, Min Zhuo^a, Bo
Chen^{b*}, and Shuang Li^{a*}

^aSchool of Biology and Biological Engineering, South China University of
Technology, Guangzhou 510006, China

^bBeijing Evolyzer Co., Ltd., Beijing 101300, China

*Corresponding authors:

Shuang Li, School of Biology and Biological Engineering, South China University
of Technology, Higher Education Mega Center, Guangzhou 510006, China, E-mail:
shuangli@scut.edu.cn, Tel/Fax: +86 20 3938 0629

Bo Chen, Beijing Evolyzer Co., Ltd., 28 Yuhua Rd., Airport Industrial Zone B,
Beijing 101300, China, Email: chenbo@evolyzer.com, Tel: +86 10 6457 4198

Contents

Fig. S1 Optimal flux distribution for valencene production in <i>S. cerevisiae</i>	3
Fig. S2 Batch fermentation profiles of the mannitol-assimilating strain during valencene production.....	4
Fig. S3 The assimilation of mannitol requires for respiration.....	5
Fig. S4 The transcriptional levels of the gene TDH3 of BN-01A and BN-91A on glucose and mannitol compared to those in BN-00 on glucose.....	6
Fig. S5 The transcriptional patterns of genes involving in MVA pathway of the <i>TUP1</i> site mutant strains BN-01A and BN-01M and their parental strain BN-00.....	7
Table S1 Strains used in this study.....	8
Table S2 Plasmids used or constructed in this study.....	10
Table S3 Primers used in this study.....	12
Table S4 Possible binding site of the transcriptional factors GIS1 in the upstream of the genes involved in mannitol assimilation.....	17
Notes and references.....	18

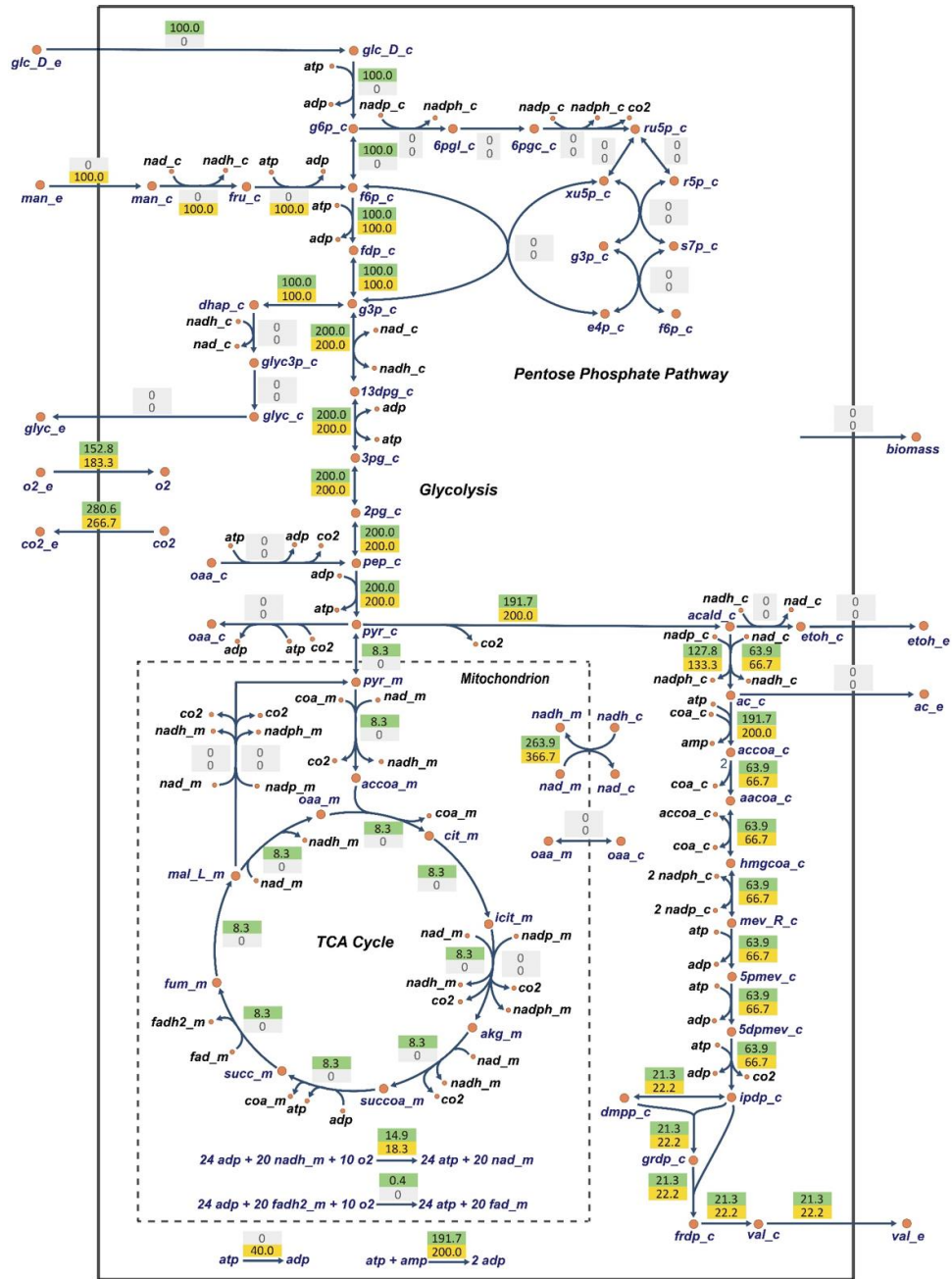


Fig. S1 Optimal flux distribution for valencene production in *S. cerevisiae*. A comparison of the theoretical flux distributions for maximum valencene yield on glucose (upper values) and mannitol (lower values). The values indicated the relative molar fluxes (mmol/gDCW/h, DCW = dry cell weight) normalized to glucose or mannitol uptake. Green and yellow reactions respectively represented the active reactions on glucose and mannitol metabolism, while grey reactions are the inactive ones. The metabolites presented in mitochondria, cytoplasm and extracellular were distinguished by the suffixes of “m”, “c”, “e”.

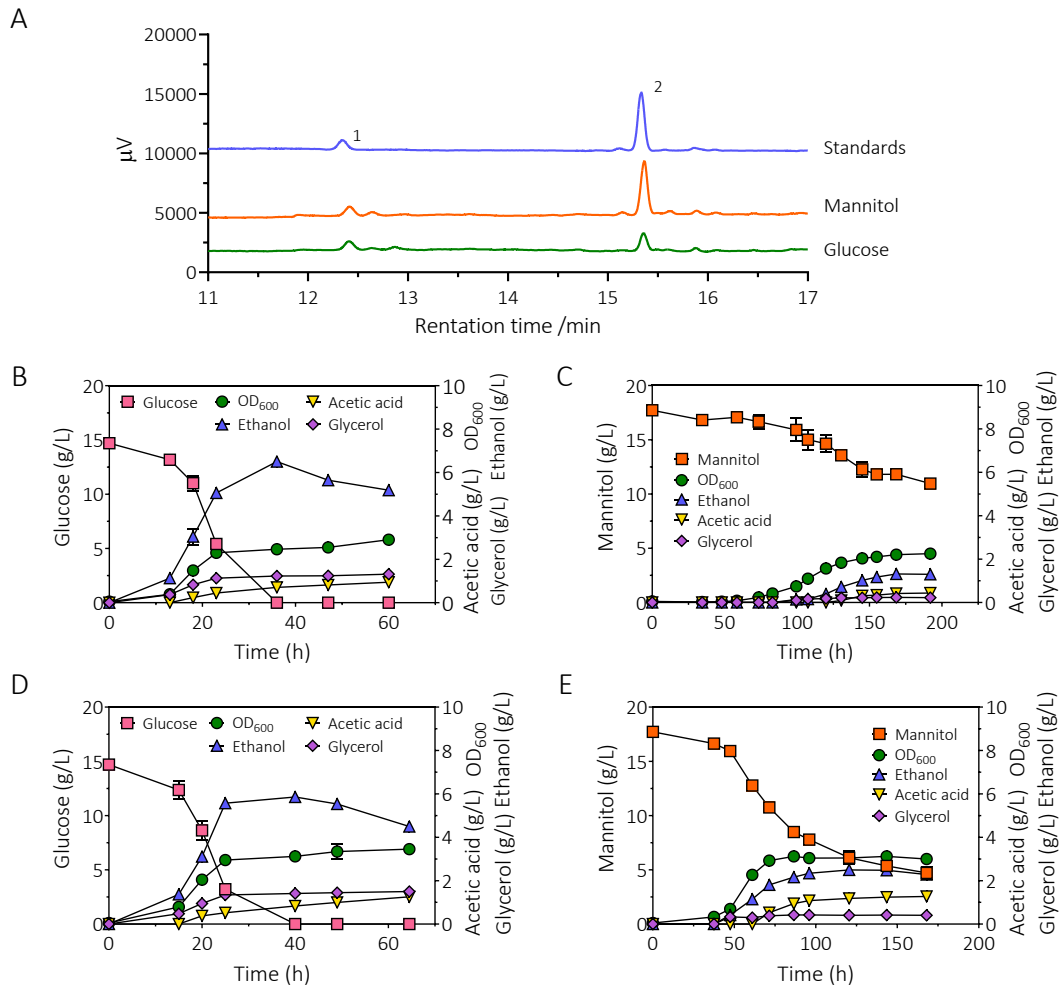


Fig. S2 Batch fermentation profiles of the mannitol-assimilating strain during valencene production. **A.** GC-FID chromatogram patterns of the products of BN-91A on glucose and mannitol as well as the standard sample. Peak 1 and 2 represented the internal standard isolongifolene and valencene, respectively. **B&C** Profiles of the strain BN-01A on glucose (B) and mannitol (C) medium. **D&E** Profiles of the strain BN-91A on glucose (D) and mannitol (E). Experiments were performed in triplicate, and error bars represent standard deviations.

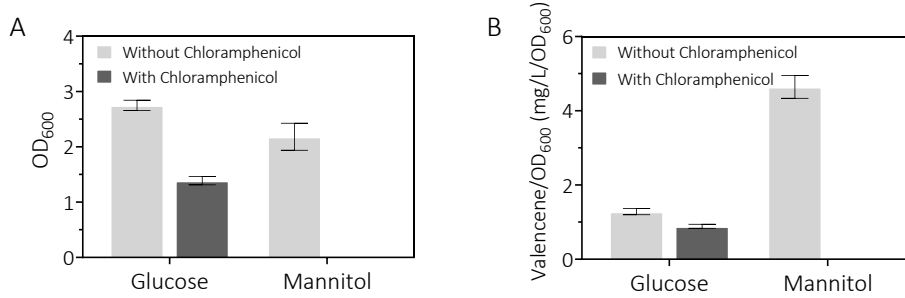


Fig. S3 The assimilation of mannitol requires for respiration. Growth (A) and valencene production (B) of the yeast BN-01A in the absence (gray column) or presence (black column) of 4 mg/mL chloramphenicol both under glucose and mannitol condition. The *S. cerevisiae* show a drop in respiratory activity in the presence of chloramphenicol, the inhibitor of the formation of mitochondrial enzymes in *S. cerevisiae*¹. Experiments were performed in triplicate, and error bars represent standard deviations.

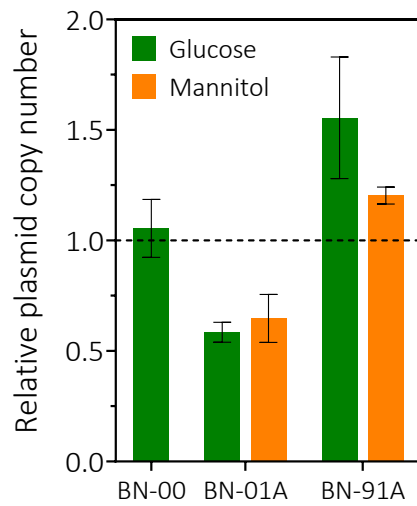


Fig. S4 The transcriptional levels of the gene *TDH3* of BN-01A and BN-91A on glucose and mannitol compared to those in BN-00 on glucose. *TDH3*, a gene coding glyceraldehyde-3-phosphate dehydrogenase on chromosome, were controlled by the same promoter P_{TDH3} with *CnVS*. The transcriptional level was quantified by RT-qPCR analysis and normalized to the *ACT1* gene. The transcriptional level of BN-00 on glucose was set to 1 as a control. Mean values and standard deviations of biological triplicates are shown.

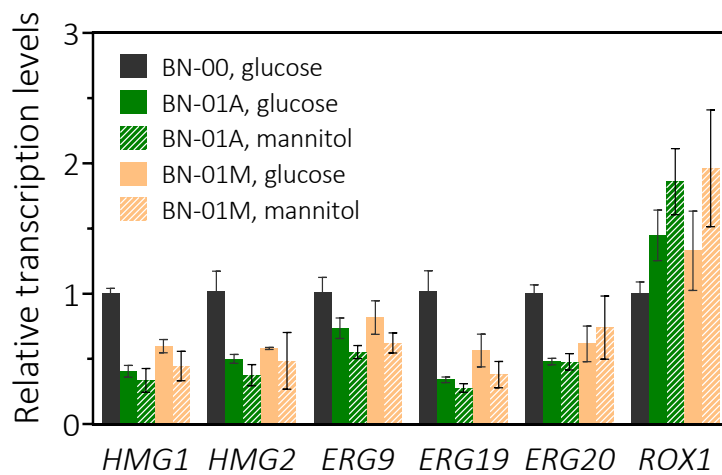


Fig. S5 The transcriptional patterns of genes involved in the MVA pathway of the *TUP1* site mutant strains BN-01A and BN-01M and their parental strain BN-00. BN-01A and BN-01M were cultured on both glucose and mannitol media, and BN-00 was cultured on glucose medium. The transcriptional level of the indicated gene was quantified by RT-qPCR analysis and normalized to the *ACT1* gene. Relative transcriptional level of each gene was defined as the ratio of each transcriptional level to the transcriptional level of BN-00 on glucose medium. All values presented are the means of three biological replicates, and error bars represent standard deviations.

Table S1 Strains used in this study

Strain	Description	Source
<i>E. coli</i>		
DH5 α	F ⁻ ϕ 80 <i>lacZ</i> Δ M15 Δ (<i>lacZYA-argF</i>) U169 <i>recA1 endA1 hsdR17</i> (<i>rK</i> ⁻ , <i>mK</i> ⁺) <i>phoA supE44</i> λ ⁻ <i>thi-1 gyrA96 relA1</i>	Invitrogen
<i>S. cerevisiae</i>		
BJ5464	MAT α <i>ura3-52 trp1 leu2</i> Δ 1 <i>his3</i> Δ 200 <i>pep4::HIS3 prb1</i> Δ 1.6R <i>can1 GAL</i>	ATCC [®] 208288 TM , ²
BN-00	BJ5464, containing YEplac181-P _{T_{DH3}} - <i>CnVS</i> -T _{ADH1}	³
BN-01A	Derived from BN-00, screened through ALE, <i>TUPI</i> R391X	This study
BN-01M	Derived from BN-00, <i>TUPI</i> C1117T by site-specific mutagenesis	This study
BN-01MG	Derived from BN-01M, <i>GIS1</i> T1036del by site-specific mutagenesis	This study
BN-91A	Derived from BN-01A	This study
BN-911A	BN-91A, \downarrow <i>ERG9</i>	This study

BN-912A	BN-911A, $\Delta ROX1::P_{TEF1}$ - <i>tHMG1</i> - T_{CYC1} - P_{TDH3} - <i>ERG12</i> - T_{ADH1}	This study
BN-913A	BN-912A, $\Delta BTS1::P_{TEF1}$ - <i>tHMG1</i> - T_{CYC1} - P_{PDC1} - <i>CnVS</i> - T_{SAG1}	This study
BN-914A	BN-913A, $\Delta HO::P_{SED1}$ - <i>HXT13</i> - T_{SAG1} - P_{CDC19} - <i>DSF1</i> - T_{ENO2}	This study
BN-915A	BN-914A, $\Delta ATG14::P_{PGK1}$ - <i>tPOS5</i> - T_{ENO2} - P_{PDC1} - <i>CnVS</i> - T_{SAG1}	This study
BN-915A(+)	BN-915A, $\Delta YPL062W::P_{URA3}$ - <i>URA3</i> - T_{URA3} - P_{TRP1} - <i>TRP1</i> - T_{TRP1}	This study

Table S2 Plasmids used or constructed in this study

Plasmid	Description	Reference
YEplac181	<i>S. cerevisiae</i> - <i>E. coli</i> shuttle vector, High-copy (2 μ), <i>LEU2</i> , <i>Amp</i> ^R	
YEplac181- <i>CnVS</i>	YEplac181 derived, P _{TDH3} - <i>CnVS</i> -T _{ADH1}	3
p426	p426-P _{SNR52} -T _{SUP4} , 2 μ ori, <i>URA3</i> , <i>Amp</i> ^R	Addgene
P426-Cas9	p426 derived, P _{SNR52} -T _{SUP4} -P _{TEF1} -Cas9-T _{CYC1}	This study
P426- <i>TUP1</i>	P426-Cas9 derived, P _{SNR52} -gRNA. <i>TUP1</i> -T _{SUP4} -P _{TEF1} -Cas9-T _{CYC1}	This study
P426- <i>GIS1</i>	P426-Cas9 derived, P _{SNR52} -gRNA. <i>GIS1</i> -T _{SUP4} -P _{TEF1} -Cas9-T _{CYC1}	This study
p414-Cas9	p414-P _{TEF1} -Cas9-T _{CYC1} , CEN/ARS, <i>TRP1</i> , <i>Amp</i> ^R	Addgene
P426-CL	p426 derived, p426-loxP-Ori-loxP-P _{GAL1} -Cre-T _{CYC1} -P _{SNR52} -T _{SUP4}	3
P426- <i>ERG9</i>	p426-CL derived, P _{SNR52} -gRNA. <i>ERG9</i> -T _{SUP4}	3
P426- <i>BTS1</i>	p426-CL derived, P _{SNR52} -gRNA. <i>BTS1</i> -T _{SUP4}	3
P426- <i>ROX1</i>	p426-CL derived, P _{SNR52} -gRNA. <i>ROX1</i> -T _{SUP4}	3

P426- <i>YPL062W</i>	p426-CL derived, P _{SNR52} -gRNA. <i>YPL062W</i> -T _{SUP4}	3
P426- <i>HO</i>	p426-CL derived, P _{SNR52} -gRNA. <i>HO</i> -T _{SUP4}	This study
P426- <i>ATG14</i>	p426-CL derived, P _{SNR52} -gRNA. <i>ATG14</i> -T _{SUP4}	This study
YEplac181- <i>tHMG1-ERG12</i>	YEplac181 derived, P _{TEF1} - <i>tHMG1</i> -T _{CYC1} -P _{TDH3} - <i>ERG12</i> -T _{ADH1}	This study
YEplac181- <i>tHMG1-CnVS</i>	YEplac181 derived, P _{TEF1} - <i>tHMG1</i> -T _{CYC1} -P _{PDC1} - <i>CnVS</i> -T _{SAG1}	This study
YEplac181- <i>HXT13-DSF1</i>	YEplac181 derived, P _{SED1} - <i>HXT13</i> -T _{SAG1} -P _{CDC19} - <i>DSF1</i> -T _{ENO2}	This study
YEplac181- <i>POS5-CnVS</i>	YEplac181 derived, P _{PGK1} - <i>POS5</i> -T _{ENO2} -P _{PDC1} - <i>CnVS</i> -T _{SAG1}	This study
YEplac181- <i>tPOS5-CnVS</i>	YEplac181 derived, P _{PGK1} - <i>tPOS5</i> -T _{ENO2} -P _{PDC1} - <i>CnVS</i> -T _{SAG1}	This study
YEplac181- <i>URA3-TRP1</i>	YEplac181 derived, P _{URA3} - <i>URA3</i> -T _{URA3} -P _{TRP1} - <i>TRP1</i> -T _{TRP1}	This study

Table S3 Primers used in this study.

Primer	Sequence (5'-3')	Description
ACT1-F	GTCGGTAGACCAAGACAC	Primers for Real-time quantitative PCR
ACT1-R	AGAAGGTATGATGCCAGA	
HXT13-F	ATAGCGATGGAGATGT	
HXT13-R	TCCCCGTTTATGACTT	
HXT15-F	GAGGCCTGTGTCTCCATCGCC	
HXT15-R	CACAAGAATACCTGTGATCAAACG	
HXT17-F	TAACACTGCACAATGGAGAGTCC	
HXT17-R	TGAGTACCCATGGATCCTCTGG	
DSF1-F	TGTTGCTGGCTGGTTCCGTTAC	
DSF1-R	GCGGCTGCCTTCAAGGTTGG	
YNR071C-F	AGGCGTCCCCTGTTGAGAATCC	

YNR071C-R	CGTTAGGGTTGGGCTGTGTGTG	
CnVS-F	CTGAAGAAGCCACATA	
CnVS-R	AATCAAGACGGCACTA	
ALG9-F	ATCGTGAAATTGCAGGCAGCTTGG	
ALG9-R	CATGGCAACGGCAGAAGGCAATAA	
TDH3-F	ATCATCCCATCCTCC	
TDH3-R	GACTCTGAAAGCCATAC	

Cas9-F	CTAAAGGGAACAAAAGCTGGCATAGCTTCAAATGTTTCTA	For creation of <i>TUPI</i> and <i>GIS1</i> mutant
Cas9-R	ATACATTATCTTTTCAAAGAGCAAATTAAGCCTTCGAGCGTCC	
gRNA-F	GCTCGAAGGCTTTAATTTGCTCTTTGAAAAGATAATGTATGAT	
gRNA-R	AGAAACATTTTGAAGCTATGCCAGCTTTTGTTCCTTTAGT	
Tong-F	TAATAATGGTTTCTTAGTATGA	
Tong-R	ACTAAGAAACCATTATTATCAT	

gRNA.TUP1-F	AAATAACACCACCACGTCCAGTTTTAGAGCTAGAAATA	
gRNA.TUP1-R	TGGACGTGGTGGTGTATTGATCATTATCTTTCACTGC	
gRNA.GIS1-F	TCTAATGAGTCGGAGCAACGGTTTTAGAGCTAGAAATA	
gRNA.GIS1-R	CGTTGCTCCGACTCATTAGAGATCATTATCTTTCACTGC	
donor. TUP1-F	CTGACGATTCTGCTGCCAATAACCATtGAAATTCGATCACTGAAAATA ACACCACCACG	
donor. TUP1-R	TTGTGGTGGTAGTAGTGGTTGTCATTGTATTGTTATCgGTGGACGTGGT GGTGTTATTT	
donor. GIS1-F	AAATGCGGCTGTGGAAACAAGAAGGAAGAGCGAAAATCTGGTCCGT TTTCAAATTTATC	
donor. GIS1-R	TATCAGTAATGGAGCtTCGTTGCTCCGCTCATTAGAATCATAAGATAAA TTTGAAAACG	
donor. ERG9-F	CTCTGACTCAGTACATTTTCATAGCCCATCTTCAACAACAATACCGACT TATCGGAAGGC	For optimization
donor. ERG9-R	GCTCGTTTAGGCACTAAACCCAAAACCGATAACGCCTTCCGATAAGT CGGTATTGTT	of the metabolic

donor. ROX1_tHMG1-R	TGGACCGCTCAAGGTGTGGAAATACCCCATAATTCAAACAGCAAATT AAAGCCTTCGA	pathway in Strain BN-91A
donor. ROX1_ERG12-F	AGACCCAAGAACGCATTTATTCTGTTCAGACAGCACTACCCATAGGG TAGGGGAATTT	
donor. BTS1_tHMG1-R	TTATAAGGTTTTGAAATCAAGCTTTCATTTTGGCTtcaAAAACGACGGC CAGTGAATTC	
donor. BTS1_CnVS-F	GTCTGGAAAATCAATGGAGGCCAAGATAGATGAGCCACACAGGAAA CAGCTATGACCAT	
donor. HO_HXT13-R	GCCAGTTAAAGGACCAGAGTGTATAAAATGTGGCGGAATCTGAATTC GAGCTCGGTAC	
donor. HO_DSf1-F	GCGCGCACCTGCGTTGTTACCACAACCTTATGAGGCCCGAACAATT TCACACAGGAA	
donor. ATG14_(t)POS5-R	AATAGTCTCATGAAGTTAGATGTTTTACGAATGAAAAAGATGAATTCG AGCTCGGTAC	
donor. ATG14_CnVS-F	TCCTTTTACTATAAATCCGCTCATTAGCTGTTCTATCCTAGCTATGAC CATGATTAC	

donor. 062_URA3-F	AGGAACTGCCGTCACATACGACACTGCCCCTCACGTAAGGGCAGAG CTTTTCAATTCAT
donor. 062_TRP1-R	CCCCGAATTTATTACGAATTTGCCACATGGTCGGTGGAGCTCAGGC AAGTGCACAAAC

Table S4 Possible binding site of the transcriptional factors GIS1 in the upstream of the genes involved in mannitol assimilation

The first base upstream the initiation codon (ATG) was indicated as the site -1, and so on.

Transcriptional factor	GIS1
Gene	
<i>HXT13</i>	-213- -217, -516- -520, -794- -798
<i>HXT15</i>	-712- -716
<i>HXT17</i>	-690- -694
<i>DSF1</i>	-871- -875
<i>MAN1</i>	-198- -202
<i>YNR071C</i>	-493- -497

Notes and references

1. M. Huang, D. R. Biggs, G. D. Clark-Walker and A. W. Linnane, *Biochim. Biophys. Acta, Nucleic Acids Protein Synth.*, 1966, **114**, 434-436.
2. E. W. Jones, *Methods Enzymol.*, 1991, **194**, 428-453.
3. H. Chen, C. Zhu, M. Zhu, J. Xiong, H. Ma, M. Zhuo and S. Li, *Microb. Cell Fact.*, 2019, **18**, 195.